Dynamic simulation of the tractor HMCVT under typical working conditions based on AMESim

Maohua Xiao[1*], Yuanfang Zhao[1], Xianhua Li[2], Ghulam Hussain[3], Shengjie Wang[4], Yejun Zhu[1]

(1. *College of Engineering, Nanjing Agricultural University, Nanjing 210031, China*;
2. *Key Laboratory of Modern Manufacturing Technology, Guizhou University, Guiyang 550025, China*;
3. *Faculty of Mechanical Engineering, Ghulam Ishaq Khan Institute of Engineering Sciences & Technology, Topi, 23460, Pakistan*;
4. *Jiangsu Yueda Intelligent Agricultural Equipment Co., Ltd., Yancheng 224004, Jiangsu, China*)

Abstract: In order to study the dynamic characteristics of hydro-mechanical continuously variable transmission (HMCVT) under ploughing and sowing conditions, a complete simulation model of HMCVT is established based on AMESim software, including mechanical transmission model, pump controlled hydraulic motor speed control model and section changing hydraulic system model. In addition, the dynamic model of tractor is established. In order to verify the correctness of the simulation model, a test-bed is established. The test of tractor running speed and the test of pump controlled hydraulic motor system were carried out on the test-bed. The test results show that the simulation model of pump control hydraulic system can correctly reflect the change of transmission ratio of pump controlled hydraulic motor, and the simulation model can reflect the actual working condition change of clutch. Thus, the correctness of the previous simulation model based on AMESim is verified. Based on the simulation model established by AMESim, the dynamic characteristics of HMCVT under ploughing and sowing conditions are studied. The results show that: Under ploughing condition, the planetary platoon will have strong impact at the moment of throttle opening and changing section. Under sowing condition, the HMCVT will have a great impact at the time of variable cross section, but the variation range of rodent force decreases and the changing trend tends to be stable.

Keywords: tractor, HMCVT, AMESim, dynamics simulation, test
DOI: 10.25165/j.ijabe.20221502.6815

Citation: Xiao M H, Zhao Y F, Li X H, Hussain G, Wang S J, Zhu Y J. Dynamic simulation of the tractor HMCVT under typical working conditions based on AMESim. Int J Agric & Biol Eng, 2022; 15(2): 102–110.

1 Introduction

Tractor as the power traction device of agricultural machinery, its power presents a growing trend[1]. At the same time, the working environment of the tractor is harsh and the operating conditions are complex and changeable[2]. In order to meet the requirements of driving speed and load under various working conditions, the gearbox of high-power tractors often needs to set many working gears. For the traditional step gearbox, the increase of gear can meet the working reliability and smoothness of high-power tractor under different working conditions, but too many gears make the gearbox structure extremely complex and the production costs become higher[3], and the manual shift operation is difficult, which also seriously limits the performance of high-power tractor[4]. In the continuously variable transmission, the hydro-mechanical continuously variable transmission (HMCVT), which realizes continuously variable transmission through parallel connection of hydraulic system and mechanical system, inherits the advantages of hydraulic continuously variable transmission and mechanical transmission with high efficiency[5-7], and is gradually recognized in the industry and applied in European and American agricultural machinery[8].

The hydro mechanical transmission system is composed of six parts: engine power input, power split mechanism, mechanical flow transmission system, hydraulic flow transmission system, power convergence mechanism and rear drive power output. The total power of the hydraulic mechanical transmission system is input from the engine, and then the mechanical power flow and hydraulic power flow are formed after the fixed shaft gear pair of the power distribution mechanism is distributed. The two power flows are coupled by the planetary gear mechanism at the power convergence mechanism and then output power through the power output device.

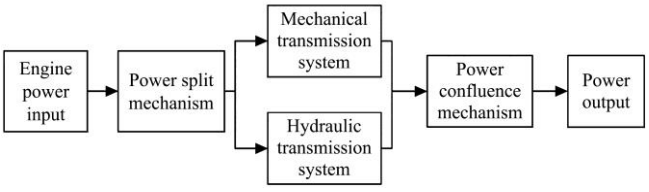

Figure 1 Principle diagram of the hydro-mechanical transmission system

In the design of High-power Tractor HMCVT, many foreign enterprises have carried out relevant research and put it into use. German RENK company has developed Audi100 proportional HMCVT, with a common ratio of 1.68, it has high efficiency and large starting torque[9]. Sundstrand has developed DMT-15 and

Received date: 2021-02-14 **Accepted date:** 2021-10-24
Biographies: Yuanfang Zhao, Undergraduate, research interests: mechanical engineering, Email: zhaoyuanfang1@hotmail.com; **Xianhua Li,** MS, Engineer, research interests: mechanical engineering, Email: xhli6@gzu.edu.cn; **Ghulam Hussain,** PhD, Professor, research interests: mechanical engineering, Email: ghulam.hussain@giki.edu.pk; **Shengjie Wang,** Bachelor, Senior Engineer, research interests: materials science and engineering. Email: ydwsj1989@126.com; **Yejun Zhu,** Assistant Professor, research interests: mechanical engineering, Email: yjzhu@njau.edu.cn.
***Corresponding author: Maohua Xiao,** PhD, Professor, research interests: mechanical engineering. College of Engineering, Nanjing Agricultural University, Nanjing 210031, China. Tel: +86-25-58606580, Email: xiaomaohua@njau.edu.cn.

DMT-25 series transmissions with power of 110 kW and 184 kW respectively[10,11]. The University of Minnesota has designed a set of HMCVT with three-layer control system, which can maintain the engine at the best working point[12]. Fendt company of Germany developed ML200 transmission, and realized the mass use in high-power tractors[13]. Steyr of Austria has developed S-matic and ML75 transmissions, which are successfully installed on VARIO700, VARIO800 and VARIO900 Series tractors[14]. ZF company of Germany has also developed ECCOM and cPOWER series transmissions[15,16].

Compared with foreign countries, although there are some related researches in China, no HMCVT has been commercialized so far. Li et al.[17] designed an HMCVT to meet the driving requirements of medium and large cotton pickers. Xu et al.[18] built an HMCVT by using computational virtual test technology, which alleviated the problems of high cost, long cycle and test site limitation due to physical test. Based on AMESim software, Zhang et al.[19] and others have carried out the modeling of HMCVT and passed the simulation test. Tai[20] designed a 2×2 stage HMCVT, and used BP neural network to optimize the transmission.

But at present, the research on HMCVT is still at the initial stage. The mechanical design and parameters can be optimized by simulation[21-23], Through the study of dynamic characteristics, we can detect whether the mechanical design is unreasonable[24]. Although the dynamic characteristics of HMCVT have been simulated in some works, the correctness of the simulation model has not been discussed. Besides, the dynamic characteristics of HMCVT loaded on tractor are often ignored in actual working conditions. Therefore, in order to establish a simulation model which can reflect the actual working conditions correctly, and analyze the typical working conditions of HMCVT, this paper designs the simulation model of HMCVT based on AMESim, the correctness of the simulation model is verified by the test-bed. The simulation experiments of ploughing and sowing conditions are carried out.

2 Construction of HMCVT dynamic model based on AMESim

The object of dynamic simulation in this paper is the HMCVT independently designed by Nanjing Agricultural University, as shown in Figure 2. This transmission scheme is a constant-ratio split-moment converging speed type[25]. The engine power is divided into two power transmissions through the fixed-axis gear pair i_1 or i_2i_3 (i_2i_3 works in forward gear) and the hydraulic power distribution gear pair i_p. One power is transmitted to the common sun gear shafts of planetary rows K_1 and K_2 through the variable displacement pump-fix displacement motor, which is a hydraulic flow; and the other power is transmitted to the planet carrier K_1 and the ring gear K_2 through the fixed shaft gear pair (the planet carrier of K_1 and the gear ring of K_2 are firmly connected), which is the mechanical flow. The hydraulic flow and mechanical flow converge in the planetary row K_1 and K_2, and then the combined flow force is transmitted to ring gear of K_1 or planet carrier K_2. Finally, by separately controlling the engagement of wet clutches C_1, C_2, and C_3, the power can be transmitted to the output shaft. In this process, stepless speed regulation can be realized in each section by controlling the displacement ratio of the variable pump.

The software AMESim has a standard control system model that visually reflects the model connection and it is widely applied in fluid, mechanical, and thermal analysis[26,27]. In this chapter, AMESim software is used to model the HMCVT.

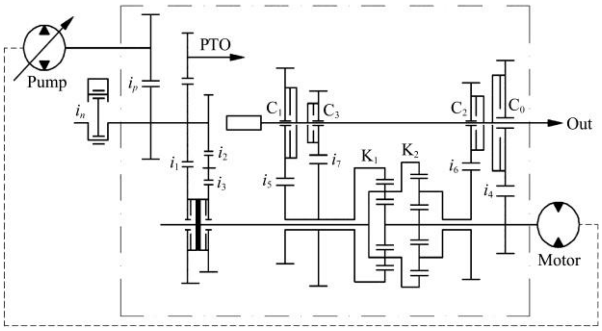

Figure 2 Independent designed HMCVT scheme

2.1 Model construction of mechanical system of HMCVT

The mechanical system is composed of fixed shaft gear and planetary gear[28]. In the simulation model, the fixed shaft gear calls the rotary mechanical reducer module from the Powertrain library. The planetary gear mechanism calls the complete planetary geartrain module from the Powertrain library and the moment of inertia is set from the rotary load module of the machine library. The planet row model is shown in Figure 3.

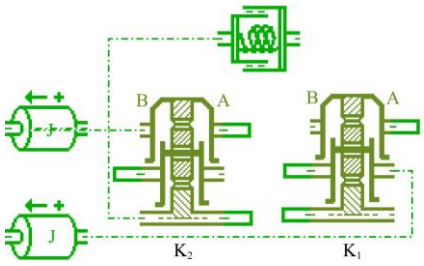

Figure 3 The model of gear transmission

2.2 Model construction of pump controlled hydraulic motor system

Pump controlled hydraulic motor system of HMCVT is composed of variable displacement pump, fix displacement motor, overflow valve and other auxiliary parts[29,30].

The pump04 [PU003C] module is selected from the Hydraulic library as the variable pump model, and motor02[M0001C] model is selected from the Hydraulic library as the fix displacement motor model. Then, presscontrol01[rv00-1] module is selected from the Hydraulic library as the model of the overflow valve, which is used to control the oil pressure.

Based on the pump, motor and overflow valve models above, signal module is selected from 'signal and control' library, and continuous signal is applied instead of proportional electromagnet to control variable pump swash plate, so as to realize the change of oil supply direction and displacement. In addition, the corresponding auxiliary components are added, and finally get the hydrostatic circuit simulation model as shown in Figure 4.

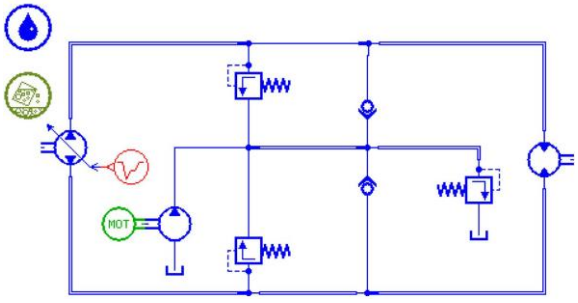

Figure 4 Simulation model of pump controlled hydraulic motor system

2.3 Model construction of shifting hydraulic system

The clutch used in the HMCVT is the wet clutch, which is mainly composed of friction disc, piston, sealing ring and piston return spring[31]. For the friction disc of the clutch, the TRDC1B_501 module of the mechanical library is applied.

The piston is established through the MAS005 and SD0000A submodules in AMESim, and the sealing ring calls USES BAFS01 model. BAP017 model is used for piston return spring, which can be used to represent the force of piston when the clutch spring is static.

The proportional valve is established from HSV23_02 submodules, and it has directional control function. The speed regulating valve is from RV000 submodules.

Based on the models of various parts of the clutch established above, the oil circuit control[32], the corresponding signal control elements and torque output elements are also added, the simulation model of the shifting hydraulic system could be obtained, as shown in Figure 5.

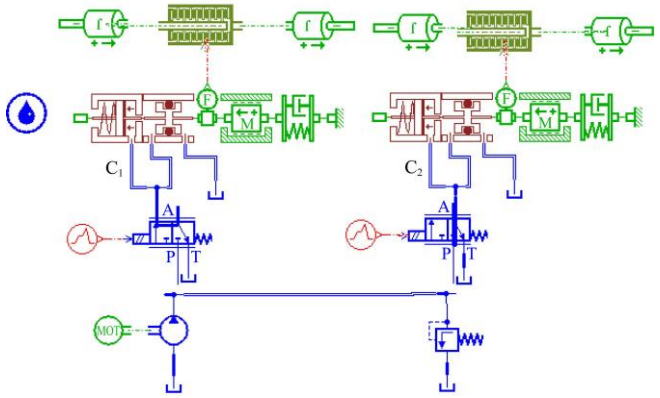

Figure 5 Simulation model of clutch shifting in HMCVT

2.4 Model construction of tractor and load

In order to simulate the actual operating conditions of tractor, it is necessary to add tractor and load model to the simulation model.

Add the vehicle model and engine model from powertrain library and customize the external load and travel speed to simulate the actual operating conditions of the tractor, as shown in Figures 6a and 6b.

The tractor rear axle drive includes the main reducer, wheel side reducer and differential, etc. The tractor rear axle drive model is established as a model with a fixed transmission ratio. The gear model selects the reducer module of the machinery library, and the established tractor rear axle model is shown in Figure 6c.

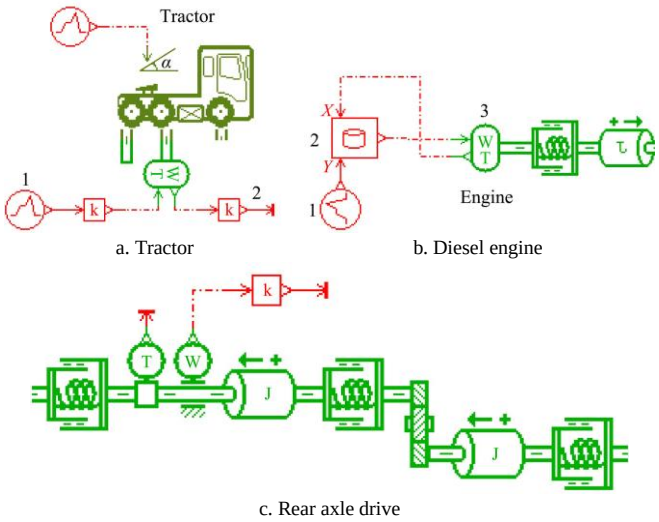

Figure 6 Tractor and load model

2.5 Model construction of HMCVT

According to the mechanical system model, pump controlled hydraulic motor system model, shifting hydraulic system model, tractor and load model, the simulation model of HMCVT is obtained, as shown in Figure 7.

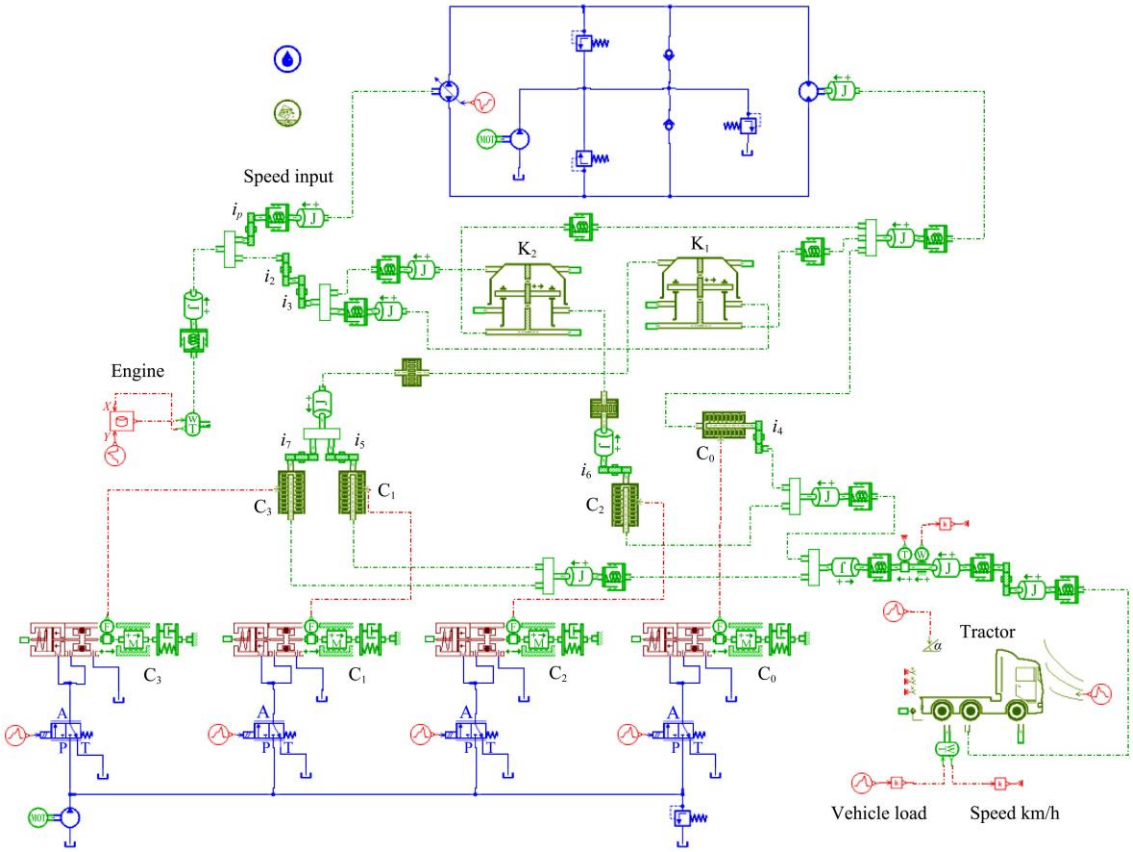

Figure 7 HMCVT simulation model

3 Validation of HMCVT model

In order to verify the correctness of the HMCVT simulation model based on AMESim in the previous chapter, this chapter builds the HMCVT test-bed according to the simulation model.

3.1 Construction of test bed

The test bed consists of pump control hydraulic motor system and clutch shifting system. The test bed of pump controlled hydraulic motor speed control system mainly studies the relationship between the transmission ratio of pump controlled hydraulic motor speed control system and the power on voltage of proportional electromagnet. The clutch shifting system mainly studies the charging characteristics of the clutch.

The test bed can be divided into transmission system and control system in function. The schematic diagram of the transmission system is shown in Figure 8.

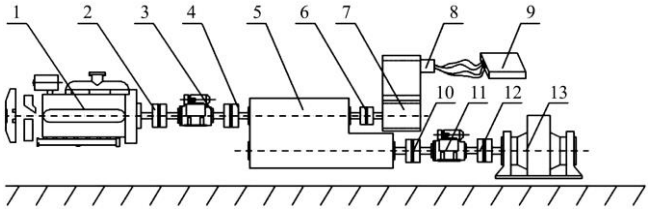

1. Engine 2,4,6,10,12. Coupling 3,11. Speed torque sensor 5.HMCVT 7. Pump controlled hydraulic motor system 8. Proportional electromagnet 9. DC regulated power supply 13. Dynamometer

Figure 8 Transmission schematic of test-bed

The engine, gearbox, speed torque sensor and dynamometer are connected by coupling. The pump controlled hydraulic motor system is controlled by a separate oil circuit, and the hydraulic oil is supplied by the hydrostatic tank. The clutch shifting system also uses a separate oil circuit control, which is mainly controlled by the electromagnetic directional valve. The test bed is shown in Figure 9. The main component hardware of the test bench is shown in Table.1.

1. Dynamometer 2,4. Speed torque sensor 3. HMCVT 5. Engine

Figure 9 Hardware design of test-bed

Table 1 Main part parameters of test-bed

Part name	Model	Main performance parameters	Place of origin
Diesel engine	WP6T180E21	132.5 kW, 2200 r/min	Weifang
Speed torque sensor	JC3A	Rated torque 5000 N·m	Xiangyi power test instrument
Eddy current dynamometer	GWD160	The rated torque is 600 N·m and the absorbed power is 160 kW	Xiangyi power test instrument
HMCVT	HMCVT-180	Matching with 180 HP tractor	Independent design

The pump controlled hydraulic motor system is shown in Figure 10. The displacement of the variable displacement pump is controlled by controlling the current change of the proportional electromagnet of the variable displacement pump and the inclination angle of the swash plate. The control current of the proportional electromagnet is 225-400 mA, and the resistance is 24 Ω. Therefore, the DC regulated power supply is used to control the proportional electromagnet voltage from 5 to 14 V. The parameter of variable pump and quantitative motor is listed in Table 2.

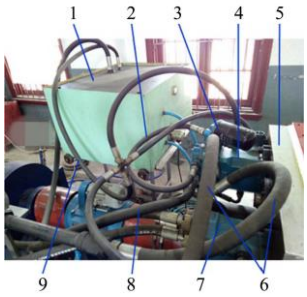

1. Fuel tank 2. Make up oil pipe 3. Filter 4. Variable displacement pump 5. Gearbox 6. High pressure oil pipe 7. Quantitative motor 8. Oil return pipe 9. Oil suction pipe

Figure 10 Test oil circuit diagram of pump controlled hydraulic motor system

Table 2 Parameter of variable pump and quantitative motor

	Rated displacement /cm^3·rev^{-1}	Rated speed /r·min^{-1}	Rated pressure /bar	Torque /N·m	Power /kW
Variable pump	54.8	3300	420	220-350	75
Quantitative motor	54.8	3300	420	199-366	75

3.2 Experimental verification

In this section, through the use of the above test bench, the test of tractor running speed and the test of pump controlled hydraulic motor system are carried out, and the test and simulation results are compared to verify the correctness of the HMCVT simulation model based on AMESim.

3.2.1 Test of tractor running speed

The specific experimental steps of tractor running speed test are as follows:

1) Start the diesel engine and make it idle for 15 min to ensure the stability of the operation condition;

2) Keeping the throttle opening of diesel engine unchanged, HMCVT is controlled by the control system to complete the shift operation, so that the tractor speed can change from 0-30 km/h;

3) The tractor speed data collected by the data acquisition card is processed, and the change trend of tractor speed with time is obtained, the comparison of test and simulation results is as shown in Figure 11.

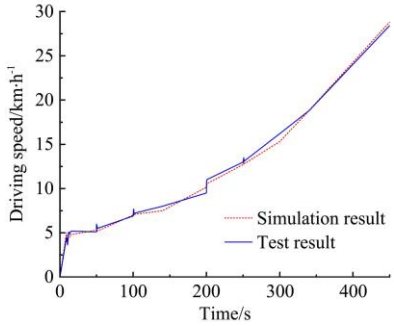

Figure 11 Tractor running speed

3.2.2 Test of pump controlled hydraulic motor system

The specific experimental steps of pump controlled hydraulic motor speed regulation test are as follows:

1) Start the diesel engine and make it idle for 15 min to ensure the stability of the operation condition. Open the three-phase asynchronous motor to run for 5 min, adjust the relief valve and speed control valve to make the oil pressure of main oil circuit 5MPa and the flow of main oil circuit 5 L/min.

2) On the clutch control panel, control C1 clutch to be engaged, and then make C1 clutch to be disengaged and C2 clutch to be engaged. Repeat this step three times;

3) The data of transmission ratio of pump control hydraulic motor collected by data acquisition card are processed, and the diagram is made by Matlab to get the following transmission ratio of pump control hydraulic motor system and the change trend of electromagnet voltage. As shown in Figure 12;

4) The clutch oil pressure data collected by the data acquisition card is processed, and the following clutch oil pressure change trend is obtained through Matlab. The charging characteristics of the clutch are shown in Figure 13, and the change of oil pressure when the clutch is switched from C1 to C2 is shown in Figure 14.

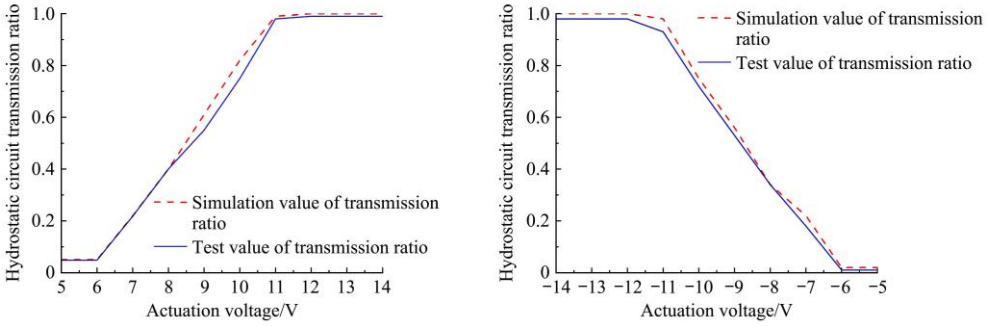

a. Positive bias b. Reverse bias

Figure 12 Relationship between the pump control hydraulic motor system transmission ratio and the proportion of the electromagnetic shunt voltage

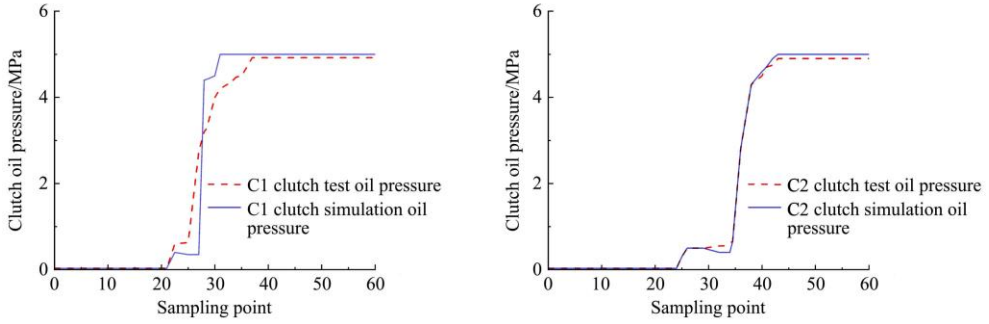

a. Clutch C1 oil pressure change b. Clutch C2 oil pressure change

Figure 13 Oil filling characteristics of clutch

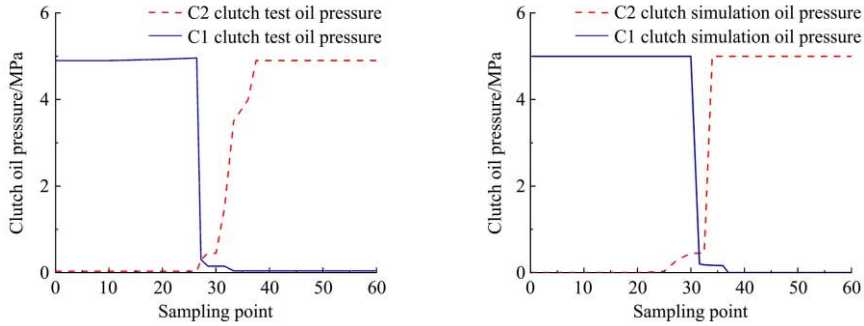

a. Shifting from C1 to C2 in test b. Shifting from C1 to C2 in simulation

Figure 14 Pressure curve during shift of clutch 1 to 2 base on simulation

3.3 Analysis of experimental results

The conclusion can be drawn by analyzing Figure 11:

1) By comparing the simulation results with the test results, we can see that the trend of the two is basically the same, which proves the correctness of the simulation model.

2) HMCVT can achieve stepless speed regulation in the speed range, and the speed changes smoothly in the low speed section, which is suitable for tractor low speed operation in the field; The speed of high-speed section increases rapidly, which is suitable for road transportation.

It can be seen from Figure 12 that the change trend of transmission ratio and power on voltage of proportional electromagnet test bench and simulation results of pump controlled hydraulic motor is similar regardless of positive or negative bias of variable displacement pump, and basically presents a consistent linear relationship. This proves that the simulation model of pump control hydraulic system built previously can correctly reflect the working condition change of pump control hydraulic motor transmission ratio in actual work.

According to the test and simulation results in Figure 13 and Figure 14, the following conclusions can be drawn:

1) The results of oil pressure change and simulation model of clutch C1 and C2 are basically similar. The clutch engagement process is oil charging, pressure boosting, pressure maintaining and

other stages, which is consistent with the clutch engagement process in reference[33];

2) The results show that the change of oil pressure in the bench test is similar to that in the simulation model, and the change of oil pressure is faster when the clutch C1 is switched to C2;

3) Through the analysis and comparison of clutch bench test and simulation results of oil pressure change, it is found that the simulation model can reflect the actual working condition change of clutch, which verifies the correctness of the previous simulation model based on AMESim.

4 Simulation analysis of typical working conditions of tractor

It can be seen from reference[34] that the working speed of 4-15 km/h in the working life cycle of tractor accounts for 75%. In this life cycle, heavy load ploughing and light load sowing are two typical working conditions of tractor field operation. Because of the different loads and the different tractive forces, the two working conditions have different effects on the performance of tractor gearbox. The dynamic simulation analysis of planetary array under different working conditions has important guiding significance for the design of gearbox. According to the HMCVT simulation model based on AMESim, the dynamic simulation of the above two typical working conditions is carried out in this chapter.

4.1 Simulation analysis of ploughing condition

Before the simulation analysis, the load of ploughing condition is analyzed. When the tractor is working in ploughing condition, its traction resistance P can be expressed as:

$$P=f G+k_0 a b+k_1 a b v^2 \quad (1)$$

where, G is the weight of plow, kg; f is the friction coefficient; k_0 is static resistance coefficient, kg/cm^2; a is tillage depth, cm; b is tillage width, cm; k_1 is dynamic resistance coefficient, kg s^2/m^4, related to soil type, plough characteristics, bulk density and tillage speed; v is ploughing speed, m/s.

The specific parameters of the moldboard plow used in the simulation analysis are: the width is 80 cm, the mass is 1710 kg, the comprehensive friction coefficient between plow and soil is 0.4, ploughing depth is 40 cm. The ploughing conditions were simulated twice as follows:

Simulation 1: Keep the throttle opening at 1, start with Hm1, and the displacement ratio is e ∈(–1, 1) The simulation time was 10 s, the initial ploughing depth was 10 cm, and then the ploughing depth was 10 cm in the second, fourth, sixth and eighth second.

Simulation 2: Through calculation and analysis, it is known that the transmission load is 47.068 kN·m when the tractor is in ploughing heavy load condition. The simulation results show that the tire load is 47.068 kN·m, starting from HM1, the throttle opening is 0.6 and 1 respectively, and the displacement ratio range is e ∈(–1, 1) and e∈(1, –1), the simulation time is 10 s, and the segment is changed in the fifth second.

After the above simulation for each 10 s, the time-varying diagrams of planet carrier speed, sun gear speed, ring gear speed and engine output speed are obtained:

The change trend of planetary frame and sun wheel speed, ring gear torque and engine output speed obtained by simulation based on AMESim software is shown in Figure 15. The engine speed changes with throttle opening, the speed of planetary carrier and solar wheel increases with the increase of engine speed, and the speed of solar wheel is also affected by displacement ratio e. From the simulation 1 curve, it can be seen that the torque of the ring gear increases with the increase of the ploughshare depth.

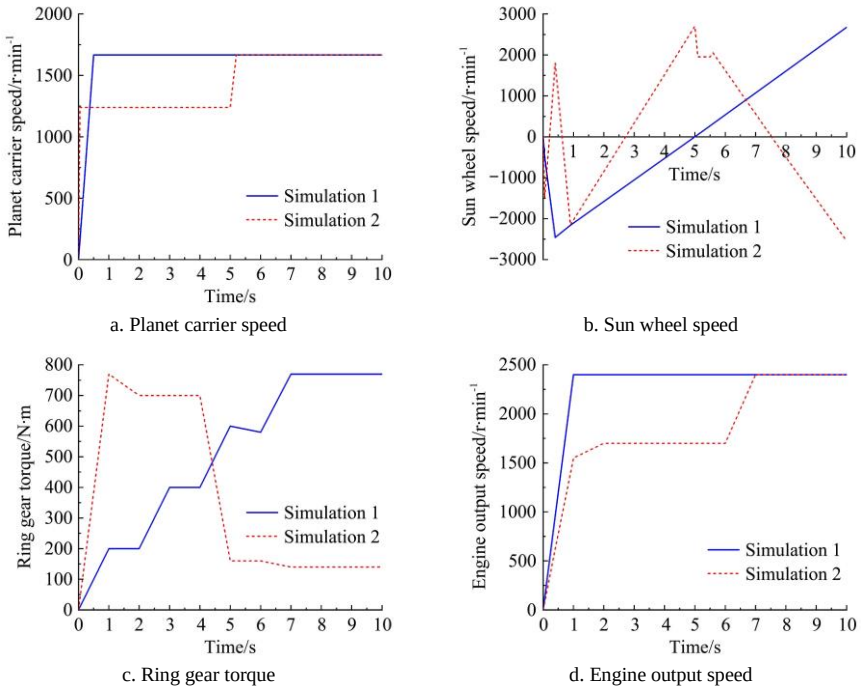

a. Planet carrier speed

b. Sun wheel speed

c. Ring gear torque

d. Engine output speed

Figure 15 Simulation parameters of AMESim in pear cultivation condition

Figures 16 and 17 show the change of planetary meshing force under ploughing condition. It can be seen from Figure 16 that with the increase of Plowshare penetration depth and load, the internal and external meshing forces of planetary gear also show a larger trend. The range of internal force was 0-11430 kN, with an average of 1305 kN; The range of external force was 0-7291 kN, with an average of 53.449 kN. It can be seen that when the plowshare reaches the specified depth from the beginning of operation, the impact force of planetary gear gradually increases, the impact of planetary gear gradually increases, the vibration of planetary gear increases, and the impact transmitted to the gearbox also increases. Figure 17 shows the change of meshing impact

force of planetary gear when changing engine throttle and changing section during ploughing operation. The change of internal and external meshing force of planetary gear has great impact at the moment of changing section during ploughing operation. The maximum value of internal meshing force of planetary gear is 16870 kN, the minimum value is –18190 kN, and the average value is 94.448 kN; The maximum and minimum of external engagement force were 5759 kN and –7261 kN, respectively, with an average of 50.783 kN. It can be seen that the segment change has a great impact on the planetary gear meshing. Based on the above simulation 1 and 2, it can be seen that the planetary row is subject to great impact force during ploughing operation. If the meshing force between the teeth is too large, the gear teeth will break, which will affect the accurate transmission of power.

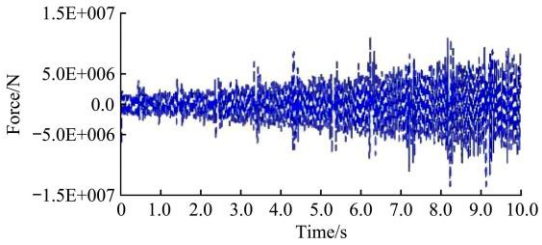

a. Internal force

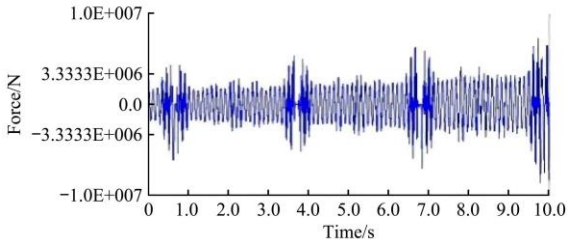

b. External force

Figure 16 Internal and external meshing force of planet gear in pear cultivation condition simulation 1

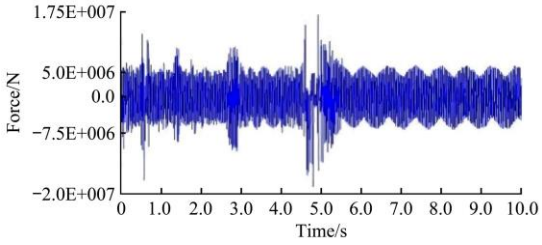

a. Internal force

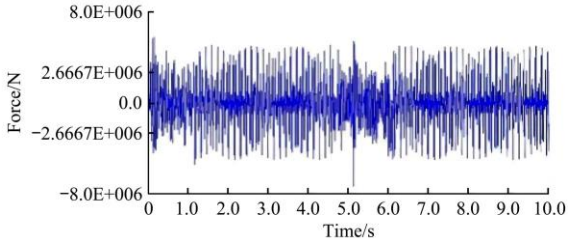

b. External force

Figure 17 Internal and external meshing force of planet gear in pear cultivation condition simulation 2

4.2 Simulation analysis of seeding condition

The empirical formula of traction resistance P_t under sowing condition is:

$$P_t = c\ k \quad (2)$$

where, c is broadcast, m; k is average resistance per mu, N/m.

The resistance per unit width is set as 1350 N and the seeding amplitude is 4 m. The output load is 5400 N·m under the seeding condition. The seeding conditions were simulated twice as follows:

Simulation 1: Drag the tire, set the load 5400 N·m, start with HM1, the throttle opening is 0.3 and 0.6 respectively, displacement ratio range is e∈ (–1, 1), the simulation time is 5 s, and the throttle opening is changed at 2.5 s;

Simulation 2: The tractor tire is set with 5400 N·m load, starting with HM1, the throttle opening is 0.3 and 0.6 respectively, and the displacement ratio range is e ∈ (–1,1) and e∈ (1, –1), the simulation time is 5 s, change the throttle opening at 2.5 s and change the section at the same time.

The planetary carrier speed, sun gear speed, ring gear torque and engine speed obtained by AMESim system dynamics software simulation are shown in Figure 18. The results show that the planetary carrier speed and sun gear speed have impact when the engine throttle opening changes, and the ring gear torque also fluctuates when the engine throttle opening changes.

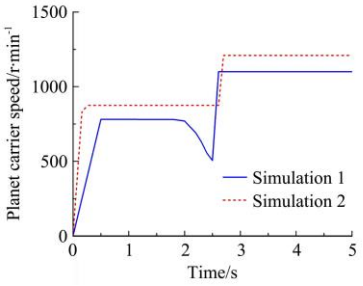

a. Planet carrier speed

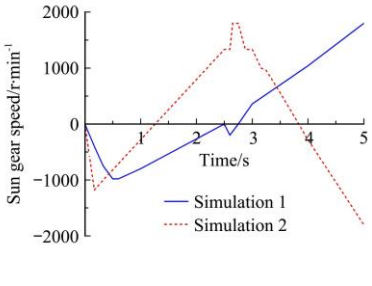

b. Sun gear speed

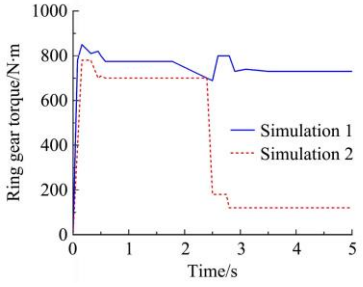

c. Ring gear torque

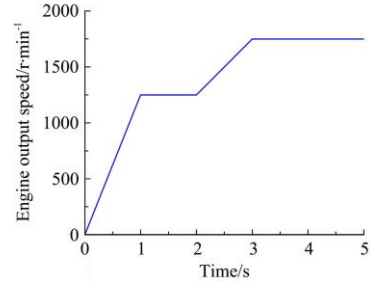

d. Engine output speed

Figure 18 Simulation parameters of AMESim in sowing condition

Figures 19 and 20 show the changes in the internal and external meshing forces of the planetary gear. It can be seen from Figure 19 that the internal and external meshing forces of the planetary gear have a great impact at the moment when the throttle opening of the engine changes. The maximum value of the internal meshing force is 16010 kN, the minimum value is –20010 kN, and the average value is 92.969 kN; The maximum value of external meshing force is 4034 kN, the minimum is –496.1 kN, the average was 56.407 kN; The internal and external engagement force increases with the increase of throttle opening. Figure 20 shows the impact of planetary gear teeth during changing sections under seeding condition. At the moment of changing sections, the internal and external meshing forces of planetary gear are in 2.5-3.5 s, which has a great impact, and then the change amplitude of meshing force decreases and the change trend tends to be stable.

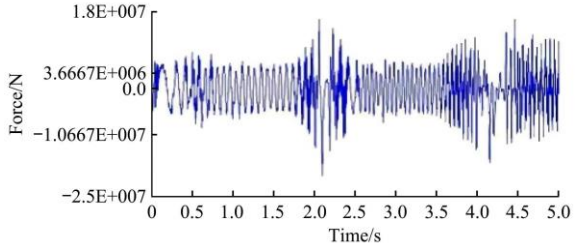

a. Internal force

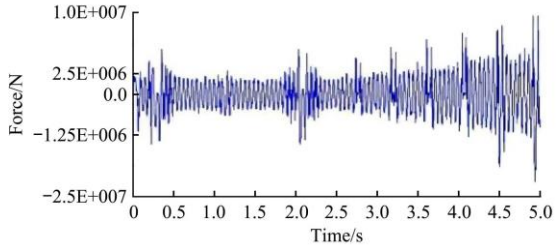

b. External force

Figure 19 Internal and external meshing force of planet gear in sowing condition simulation 1

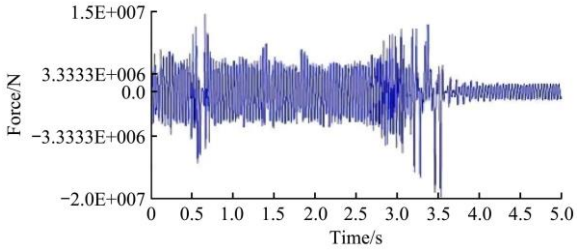

a. Internal force

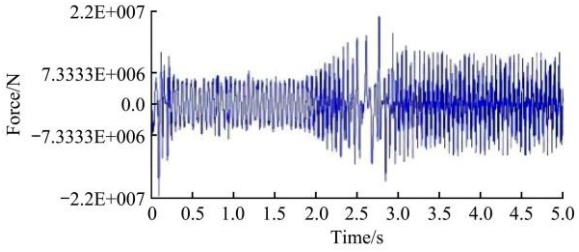

b. External force

Figure 20 Internal and external meshing force of planet gear in sowing condition simulation 2

5 Conclusions

Based on AMESim software, the dynamic simulation model of HMCVT is established, and the test bench is built according to the model. The experimental data show that the dynamic simulation model of HMCVT based on AMESim software can correctly reflect the real operation condition of HMCVT.

Based on the above model, the dynamic simulation of tractor ploughing and sowing conditions was carried out. The results show that:

1) When the engine throttle opening increases, the engine speed increases, and the planetary carrier and sun gear speed also increases. When the engine throttle opening changes instantaneously, the planetary carrier speed and the sun gear speed fluctuate, the planetary carrier and the sun gear impact, and the ring gear torque also fluctuates when the engine throttle opening changes.

2) When HMCVT is in ploughing condition, with the increase of plowshare depth, the torque of ring gear increases gradually, the impact force of planetary gear increases gradually, the impact of planetary gear increases gradually, the vibration of planetary gear increases, and the impact transmitted to gearbox also increases. During the ploughing process, the internal and external meshing forces of the planetary gear change instantaneously at the moment of changing section, which has a great impact on the HMCVT planetary array.

3) When HMCVT is in seeding condition, with the instantaneous change of engine throttle opening, the internal and external meshing forces of planetary gear change instantaneously, and HMCVT planetary array has a great impact. In the process of seeding, a great impact occurred at the moment of changing section, but then the change amplitude of meshing force decreased and the change trend tended to be stable.

In this study, the change trend of meshing force and the location and timing of impact of HMCVT internal gear under typical working conditions are proved. It is conducive to the optimal design of HMCVT in the future, and can also provide a theoretical basis for the design of HMCVT control system.

Acknowledgements

The research is funded partially by the Jiangsu International Cooperation Project (Grant No. BZ2021007), the Modern Agricultural Machinery Equipment and Technology Promotion Project in Jiangsu Province (Grant No. NJ2021-06), the Nanjing International Science and Technology Cooperation Project (Grant No. 202002049), the Xuzhou key research and development projects (Grant No. KC21136) and The Fundamental Research Funds for the Central Universities(Grant No. KYGD202105).

[References]

[1] Rossetti A, Macor A. Multi-objective optimization of hydro-mechanical power split transmissions. Mechanism and Machine Theory, 2013; 62: 112–128.

[2] Lloyd R. High efficiency, hydro-mechanical passenger vehicle transmission using fixed displacement pump/motors and digital hydraulics. SAE International Journal of Passenger Cars-Mechanical Systems, 2012; 5(2): 833–855.

[3] Tomiji W. E221 hydro-mechanical hybrid transmission for wind/wave power plant. The Proceedings of the National Symposium on Power and Energy Systems, 2015; 20: 327–330.

[4] Oledzki W J. Split power hydro-mechanical transmission with power circulation. Journal of the Chinese Institute of Engineers, 2018; 41(4): 333–341.

[5] Rossetti A, Macor A. Control strategies for a powertrain with hydromechanical transmission. Energy Procedia, 2018; 148: 978–985.

[6] Kim J. Design of power split transmission: Design of dual mode power split transmission. International Journal of Automotive Technology,

2010; 11(4): 565–571.
[7] Matmurodov F. Mathematical modeling of the transfer of energy forces from the engine through hydro transmission and hydro differential to executive bodies. World Journal of Mechanics, 2019; 9(5): 105–112.
[8] Ivanov K S. Creation of adaptive-mechanical continuously variable transmission. Applied Mechanics and Materials, 2013; 2776: 63–70.
[9] Zheng X Z, Sun W. Research overview of hydro-mechanical continuously variable transmission. Mechanical Engineering, 2017; 7: 37–39.
[10] Latson D M, Gordanier M, Dorgan R J, Rio R L. A hydromechanical transmission development. SAE Technical Paper 670932, 1967; doi: 10.4271/670932.
[11] Troin P E, Gostomski V G. Application consideration with the Cummins Sundstrand DMT-25 hydro-mechanical transmission. SAE paper 750732, 1975; pp.179-184. doi: 10.4271/750732.
[12] Li P Y, Mensing F. Optimization and control of a hydro-mechanical transmission based hybrid hydraulic passenger vehicle. 7th International Fluid Power Conference, Aachen, Germany, March, 2010; pp.1–12.
[13] Brenninger M M. Fendt vario CVT in agricultural tractors. SAE Technical paper 2007-01-4205, 2007. doi: 10.4271/2007-01-4205.
[14] Rahman M, Hudha K, Kadir Z A, Amer N H, Aparow V R. Modelling and validation of a novel continuously variable transmission system using slider crank mechanism. Int. J. of Engineering Systems Modelling and Simulation, 2018; 10(1): 49–61.
[15] Molari G, Sedoni E. Experimental evaluation of power losses in a power-shift agricultural tractor transmission. Biosystems Engineering, 2008; 100(2): 177–183.
[16] Zhang Z M, Zhang Y L, Li R C, Xu J K, Cui H Y. Research on ZF ECCOM hydro mechanical stepless transmission system. Modern Manufacturing Technology and Equipment, 2017; 1: 49–51, 53.
[17] Li S, Ni X D, Bao M X, Zhao X, Han S M. Design and test of hydraulic mechanical stepless transmission test bench for cotton picker. Research on Agricultural Mechanization, 2022; 44(6): 245–250, 256.
[18] Xu J J, Zhang M Z, Wang J H, Wang J Z. Design of virtual test platform for hydro mechanical continuously variable transmission tractor. Research on Agricultural Mechanization, 2022; 44(3): 219–225.
[19] Zheng X Z, Sun W. Modeling and Simulation of hydro mechanical continuously variable transmission based on AMESim. Modern Machinery, 2017; 5: 31–34.
[20] Tai J J. High power tractor 2× Design of 2-stage hydro mechanical continuously variable transmission and research on its section changing quality. MS dissertation, Shandong Agricultural University, 2017; 72p. (in Chinese)
[21] Wei W H, Peng F X, Li Y L, Chen B R, Xu Y Q, Wei Y. Optimization design of extrusion roller of RP1814 roller press based on ANSYS workbench. Applied Sciences, 2021; 11(20): 9584–9599.
[22] Wei W H, Shen J C, Yu H P, Chen B R, Wei Y. Optimization design of the lower rocker arm of a vertical roller mill based on ANSYS workbench. Applied Sciences, 2021; 11(21): 10408–10422.
[23] Xu X M, Lin P. Parameter identification of sound absorption model of porous materials based on modified particle swarm optimization algorithm. PloS One, 2021; 16(5): e0250950. doi: 10.1371/journal.pone.0250950.
[24] Xu X M, Zhang L, Jiang Y P, Chen N. Active control on path following and lateral stability for truck–trailer combinations. Arabian Journal for Science and Engineering, 2019; 44(2):1365–1377.
[25] Linares P, Méndez V, Catalán H. Design parameters for continuously variable power-split transmissions using planetaries with 3 active shafts. Journal of Terramechanics, 2010; 47(5): 323–335.
[26] Edmunds R, Feldman J A, Hicks B J, Mullineux G. Constraint-based modelling and optimization to support the design of complex multi-domain engineering problems. Engineering with Computers, 2011; 27(4): 319–336.
[27] Yassine Z, Mohamed E M, Siham B, Medromi H. An assessment of low-cost tractor motorization with main farming implements. World Electric Vehicle Journal, 2020; 11(4): 74–74.
[28] Santiago U G, Gutierrez S U, Polinder H, Sisón A F. Torque measurements from MW wind turbine Gearboxes: a system identification approach. Journal of Physics: Conference Series, 2020; 1618(2): 1–10.
[29] He L, Guo W L, Zhu S H. Hydro-mechanical transmit performance analysis for a continuously variable transmission. Journal of Food Science and Engineering, 2016; 6(3): 121–131.
[30] Xiao M H, Zhao J, Wang Y W, Yang F, Kang J, Zhang H. Research on system identification based on hydraulic pump-motor of HMCVT. Engineering in Agriculture, Environment and Food, 2019; 12(4): 420–426.
[31] Katharina V, Hermann P, Karsten S. Running-in behavior of wet multi-plate clutches: Introduction of a new test method for investigation and characterization. Chinese Journal of Mechanical Engineering, 2020; 33(1): 160–168.
[32] Xu X M, Chen D, Zhang L, Chen N. Hopf bifurcation characteristics of the vehicle with rear axle compliance steering. Shock and Vibration, 2019; 1: 1–12, Article ID 3402084. doi: 10.1155/2019/3402084.
[33] Ho B M, Yeol B T, Rak Y Y. A strength analysis of gear train for hydro-mechanical continuously variable transmission. International Journal of Advanced Culture Technology, 2018; 6(3): 163–172.
[34] Diego S. Technical, economic, and environmental parameters of excavator-based harvester in function of engine speed and hydraulic pump flow. Croatian Journal of Forest Engineering: Journal for Theory and Application of Forestry Engineering, 2020; 41(2): 1–12.